Eq. (1) can be rewritten as

$$\frac{L_{u_n}}{\delta} Re_\delta^a = f\left(\frac{L_s}{\delta} Re_\delta^b,\ M_n\right) \qquad (2)$$

for a fixed M_∞.

The test data confirm the validity of this functional relationship. Similar to the compression ramp studies, good correlations are obtained with $a=b=1/3$. Over the limited range of α tested, L_{u_n} was found to be weakly, but linearly, dependent on M_n. Large values of L_{u_n} were observed with very weak shock waves. Figure 2 shows results obtained in the first test series, carried out at constant Re_∞. In this case $Re_\delta^{1/3}$ can be written as $Re_\infty^{1/3}\delta^{1/3}$, so the appropriate correlating parameters are

$$\frac{L_{u_n}}{\delta^{2/3}} \frac{1}{M_n} \text{ vs } \frac{L_s}{\delta^{2/3}}$$

Note that Fig. 2 axes are $cm^{1/3}$. Results from the second test series, at variable Re_∞, but with α fixed at 8 deg, are shown in Fig. 3. Since M_n is fixed, the appropriate correlating parameters are

$$\frac{L_{u_n}}{\delta} Re_\delta^{1/3} \text{ vs } \frac{L_s}{\delta} Re_\delta^{1/3}$$

In both figures, the data correlate well.

The importance of M_n has been demonstrated by Stalker.[6] In an extension of Lighthill's small perturbation analysis[7] to infinite swept flows, Stalker showed it to be the dominant parameter controlling upstream influence. His experimental upstream influences (defined as the distance normal to the isobars over which the perturbation pressure increased by the factor e), measured in skewed shock wave and forward facing swept step interactions, at a fixed M_∞ (=2.36) and Re_∞, were in overall agreement with the analysis. The current data provide further evidence of the importance of M_n.

Concluding Remarks

The results described show that a scaling technique can be developed which correlates upstream influence in sharp fin-induced shock wave turbulent boundary-layer interactions. Although the dimensional scale differs from that in swept compression ramp flows at similar flow conditions, the scale effects of changing boundary-layer thickness and Reynolds number are the same. In both cases, the scale increases with increasing boundary-layer thickness and decreasing Reynolds number.

In applying these results, a word of caution is in order. Since the tests were made at a single Mach number and over a limited range of shock wave strengths, Reynolds numbers, and boundary layers, the possible general validity of the scaling law cannot be assessed. It is likely that the empirical constants are dependent on freestream conditions. As part of a continuing research program, tests at Mach 2 will be made shortly and hopefully they will answer these questions.

Acknowledgments

This work was supported by the U.S. Air Force Office of Scientific Research under Contract F49620-80-C-0092 monitored by Dr. J. Wilson. Discussions with Dr. G. S. Settles are gratefully acknowledged.

References

[1] Horstman, C. C. and Hung, C. M., "Computation of Three-Dimensional Turbulent Separated Flows at Supersonic Speeds," AIAA Paper 79-0002, Jan. 1979.

[2] Oskam, B., Bogdonoff, S. M., and Vas, I. E., "Study of Three-Dimensional Flow Fields Generated by the Interaction of a Skewed Shock Wave with a Turbulent Boundary Layer," AFFDL-TR-75-21, Feb. 1975.

[3] Peake, D. J., "The Three-Dimensional Interaction of a Swept Shock Wave with a Turbulent Boundary Layer and the Effects of Air Injection on Separation," Ph.D. Thesis, Carleton University, Ottawa, Canada, 1975.

[4] Settles, G. S., Perkins, J. J., and Bogdonoff, S. M., "Upstream Influence Scaling of 2D and 3D Shock/Turbulent Boundary Layer Interactions at Compression Corners," AIAA Paper 81-0334, Jan. 1981.

[5] Settles, G. S., "An Experimental Study of Compressible Turbulent Boundary Layer Separation at High Reynolds Numbers," Ph.D. Thesis, Princeton University, Princeton, N.J., 1975.

[6] Stalker, R. J., "Sweepback Effects in Turbulent Boundary Layer Shock Wave Interaction," *Journal of Aerospace Sciences*, Vol. 27, No. 5, 1960, pp. 348-356.

[7] Lighthill, M. J., "On Boundary Layers and Upstream Influence: Part II—Supersonic Flows without Separation," *Proceedings of the Royal Society*, A217, 1953, pp. 478-507.

A Comparative Study of Time-Marching and Space-Marching Numerical Methods

R.N. Gupta,* J.N. Moss,† and A.L. Simmonds‡
NASA Langley Research Center, Hampton, Virginia

Introduction

RECENTLY an evaluation[1] of the three different flowfield codes[2-4] for the Jupiter entry conditions was presented. However, direct comparisons have been hampered by the fact that the three codes use different solution procedures, different computational mesh sizes, different chemical and turbulence models, different convergence criterion, as well as a different number of computational grid points along and perpendicular to the body. Even for the only common feature of radiative transport code, there are subtle differences in the spectral details of some species. Thus, for an objective evaluation of the different numerical solution methods employed by these codes, it would be desirable to select a simple no-blowing perfect-gas flowfield case for which the turbulent models are well established. The purpose of this Note is to present the results of such a study.

Analysis

The results have been obtained by employing two of the three numerical codes mentioned earlier. The first of these two is a space-marching method (perfect-gas version of HYVIS[2]) that solves the steady-state viscous-shock-layer-type equations by the method of Davis.[5] The second one is a time-marching method (perfect-gas version of COLTS[3]) that employs the time-asymptotic, two-step, finite difference method of MacCormack[6] for the solution of time-dependent viscous-shock-layer-type equations. For this study, the two methods also employ the same turbulence model[7] with and without blowing.

In addition to the prescribed surface blowing rate distribution, the boundary conditions employed along the

Received Oct. 19, 1981; revision received May 3, 1982. This paper is declared a work of the U.S. Government and therefore is in the public domain.

*NRC-Senior Research Associate, Aerothermodynamics Branch, Space Systems Division; on leave from IIT, Kanpur, India; Professor, Department of Aeronautical Engineering. Member AIAA.

†Research Leader, Aerothermodynamics Branch, Space Systems Division. Member AIAA.

‡Mathematician, Aerothermodynamics Branch, Space Systems Division. Member AIAA.

body surface are no velocity slip and temperature jump.§ The wall temperature is taken as a constant specified value. The conditions imposed at the shock are calculated by using the Rankine-Hugoniot shock relations. Further, Sutherland's equation has been used to determine the viscosity, and the coefficient of thermal conductivity is computed by assuming a constant Prandtl number.

In order to obtain a direct point-by-point comparison and to keep the same truncation error, the computations by the two schemes have been done by using identical logarithmic grid spacing[8] in the direction normal to the body to allow higher resolution near the body surface. Finally, the convergence of the solutions in both the methods is sought by requiring that the variation in the maximum value of the total-enthalpy gradient throughout the flowfield over a specified number of time steps (for the time-marching method) or consecutive global iterations (for the space-marching method) should not be greater than a prescribed value.[8]

The methods of solution employed are identical to those of Refs. 2 and 3 and, therefore, are not presented here. Briefly, since the time-marching algorithm[6] is explicit and amenable to complete vectorization, it has been programmed on a vector processor (CYBER 203). In order to speed up the calculations, the largest possible Courant-Friedrichs-Lewy (CFL) time-step size for each mesh point has been used in preference to the global minimum CFL time-step size.

Discussion of Results

First, a comparison of the predictions made by the space- and time-marching methods against the available experimental data is given. There are no experimental data available for the turbulent viscous-shock-layer problem with massive surface blowing considered in this study. For the laminar viscous-shock-layer flow at moderate Reynolds number a comparison between the predictions made by the two methods and the experimental data is contained in Fig. 12 of Ref. 9. Both the methods predict the heating rate for a 45-deg half-angle cone which compares favorably with the experimental data. For the low Reynolds number case, the predictions by the space- and time-marching methods are compared against the experimental data of Ref. 10 in Fig. 1 (where r^* is the local body radius and r_N^* is the nose radius) for a 45-deg half-angle hyperboloid. Once again, the comparison between the predictions by the two methods and the experimental data is quite good at $Re_\infty = 90$. At $Re_\infty = 1035$, the predictions depart from the experimental data. However, the predictions by the two methods compare favorably with each other.

Next, flowfield results obtained by the space- and time-marching methods are presented for the forebody of a 44.25-deg half-angle sphere-cone probe entering the Orton nominal (0.895 H_2 + 0.105 He) Jupiter atmosphere under perfect-gas assumption. Results have been obtained with and without surface blowing, assuming instantaneous transition at the first grid point downstream of the stagnation point. The freestream conditions and other parameters employed in the analysis have been taken from the peak heating entry conditions at 51.5 s for the 310-kg probe.[8] Two values of the stretching parameter β (1.1 and 1.01) were employed in the computations of the logarithmic grid distribution normal to the body surface. For the first value of β, the first grid point off the body surface is located at 0.295% of the shock standoff distance as compared with 0.05418% for $\beta = 1.01$. The various results computed by the two methods are given in Figs. 2 and 3.

Figure 2 contains the surface pressure distributions obtained by the two methods with and without surface blowing conditions. In this figure, s is the distance along the body surface nondimensionalized by the nose radius. The surface blowing rate distribution employed in the computations is also shown inset in the same figure. Except for the region near the tangency point, both the methods give comparable results. The results obtained by the two codes at the tangency point should not be taken seriously owing to the curvature discontinuity there. For an unblown shock layer, the method of characteristics[11] does give a fast pressure recovery at the tangency point similar to the one obtained by the space-marching method. The fourth-order damping employed with the time-marching method appears to smear out the effect of surface discontinuity, since a large number of global iterations is used to obtain a converged solution. It may be noticed from Fig. 2 that the surface pressure distribution is unaffected by reducing the grid stretching parameter β from 1.1 to 1.01. As will be seen later, the quantities affected most by the mesh refinement near the surface are the wall heat transfer and skin friction, as expected.

Figures 3a and 3b give the skin-friction coefficient and surface heating rates, respectively, as predicted by the two methods. Generally, the results compare more favorably over the conical flank portion than over the spherical portion or near the juncture point of the probe. Further, there is better agreement between the results obtained with a finer mesh ($\beta = 1.01$) for the unblown case. Reducing β further does not

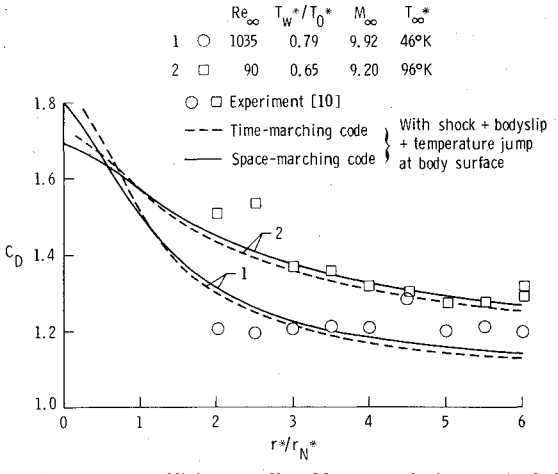

Fig. 1 Total drag coefficient predicted by two solution methods for a 45-deg half-angle hyperboloid and comparison with experimental data.

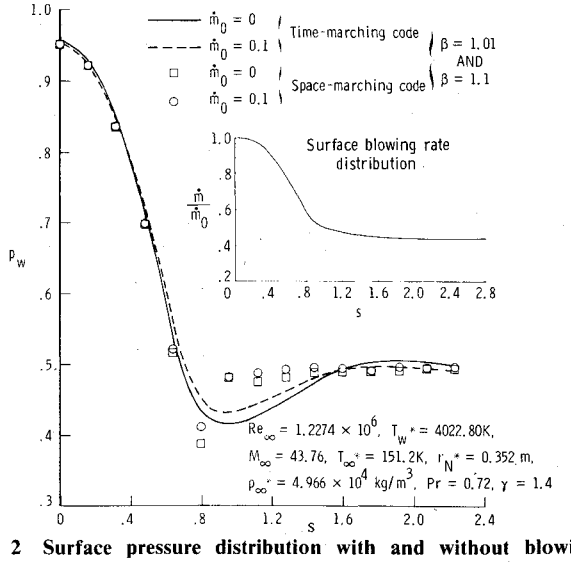

Fig. 2 Surface pressure distribution with and without blowing predicted by two solution methods for a 45-deg half-angle sphere-cone.

§For obtaining the results of Fig. 1, slip has been included both at the shock and at the body along with the temperature jump at the surface.

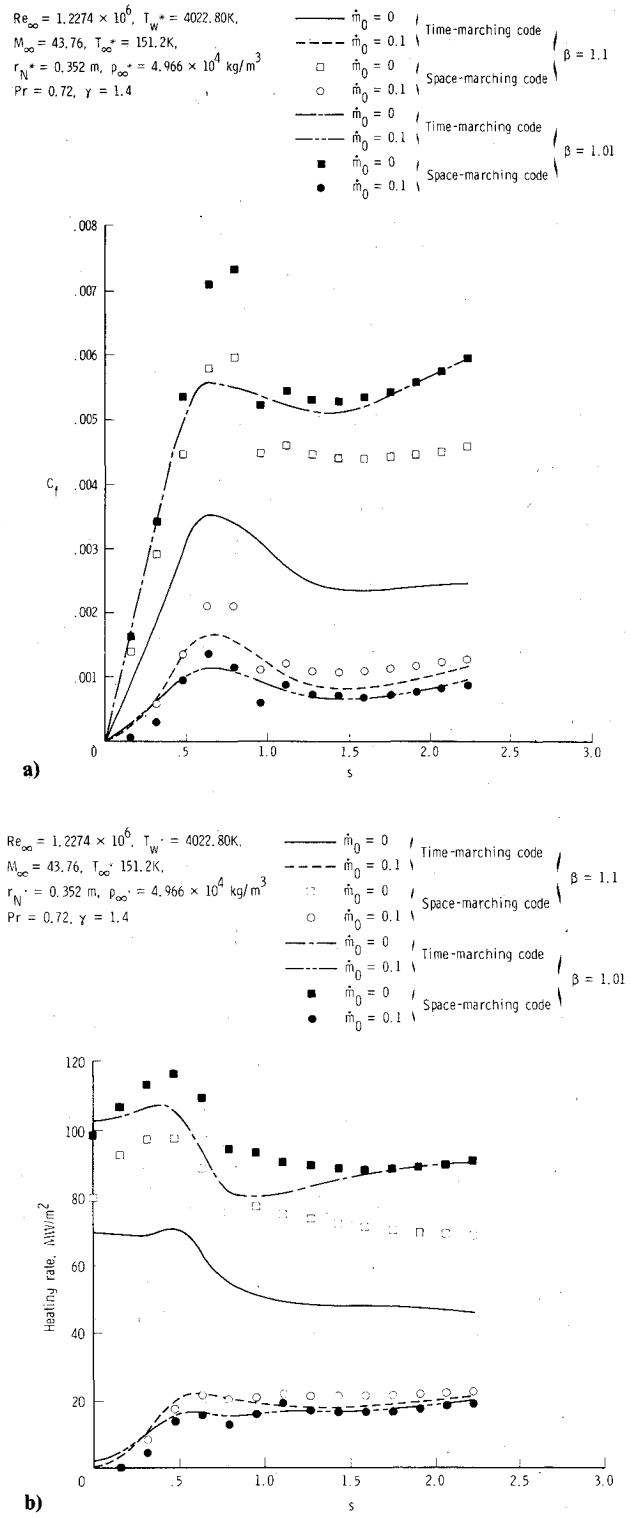

Fig. 3 Comparison of wall quantities for two solution methods for a 45-deg half-angle sphere-cone. a) Skin-friction coefficient. b) Heating rate.

result in any noticeable improvement. For the blown case, the two methods give good results for even a relatively coarse mesh ($\beta = 1.1$). Use of the largest possible value of β without jeopardizing the accuracy of the results is important, since the computational time for the blown case is reduced by almost 20% for the time-dependent method when β is increased from 1.01 to 1.1.

Computationally, in absence of blowing, the space-marching method is quite economical and gives results which compare well with the experimental data. However, with large blowing and arbitrary body shapes, the time-marching method has proved to provide solutions without the numerical instability experienced with the space-marching method. Without blowing and for analytic body shapes both methods appear equally accurate.

Further, the time-marching method has been used to predict[12] flows with large embedded subsonic regions. Some recent efforts[13] with the space-marching method have also solved such flows by making use of certain approximations to improve the initial marching profiles. The advantage of the space-marching method in such cases lies in the fact that for problems requiring more computational grid points (either owing to the large body size or large Reynolds number of the flow) the storage and computational time requirements are much less as compared to the time-marching method. Also, with the time-marching method, the computational time increases substantially if more grid points are clustered in the shear layer, whereas with the space-marching method the computational time is not significantly affected by the distribution of grid points in the shear layer. The computational time for the time-marching method, however, can be reduced substantially by employing its recent implicit analog.[14] Finally, the space-marching method would appear to provide accurate results for the problems with nonequilibrium chemistry, free from the effect of local differences in time on the final solution which is inherent in time-marching methods.[15]

Thus the choice of the numerical method is rather problem dependent. Both methods give comparable results provided that care is taken in selecting the appropriate mesh size near the body surface.

References

[1] Menees, G.P., "An Evaluation of Computer Codes for Simulating the Galileo Probe Aerothermal Entry Environment," AIAA Paper 81-1069, June 1981.

[2] Moss, J.N., "A Study of the Aerothermal Entry Environment for the Galileo Probe," AIAA Paper 79-1081, June 1979.

[3] Kumar, A., Graves, R.A. Jr., Weilmuenster, K.J., and Tiwari, S.N., "Laminar and Turbulent Flow Solutions with Radiation and Ablation Injection for Jovian Entry," AIAA Paper 80-0288, Jan. 1980.

[4] Nicolet, W.E. and Balakrishnan, A., "Methods for Predicting Off-Stagnation Point Flow Fields for Planetary Entry Probes," AIAA Paper 79-1083, June 1979.

[5] Davis, R.T., "Numerical Solution of the Hypersonic Viscous-Shock Layer Equations," *AIAA Journal,* Vol. 8, May 1970, pp. 843-851.

[6] MacCormack, R.W., "The Effect of Viscosity in Hypervelocity Impact Cratering," AIAA Paper 69-354, April 1969.

[7] Cebeci, T., "Behavior of Turbulent Flow Near a Porous Wall with Pressure Gradient," *AIAA Journal,* Vol. 8, Dec. 1970, pp. 2152-2156.

[8] Gupta, R.N., Moss, J.N., and Simmonds, A.L., "Comparison of Viscous Shock Layer Solutions by Time-Asymptotic and Steady-State Methods," NASA TM-84479, April 1982.

[9] Kumar, A. and Graves, R.A. Jr., "Numerical Solution of the Viscous Hypersonic Flow Past Blunted Cones at Angle of Attack," AIAA Paper 77-172, Jan. 1977.

[10] Little, H.R., "An Experimental Investigation of Surface Conditions on Hyperboloids and Paraboloids at a Mach Number of 10," M.S. Thesis, University of Tennessee, Tennessee, 1969.

[11] Anderson, E.C., Moss, J.N., and Sutton, K., "Turbulent Viscous-Shock-Layer Solutions with Strong Vorticity Interaction," AIAA Paper 76-120, Jan. 1976.

[12] Rizk, Y.M., Chaussee, D.S., and McRae, D.S., "Computation of Hypersonic Viscous Flow Around Three-Dimensional Bodies at High Angles of Attack," AIAA Paper 81-1261, June 1981.

[13] Thareja, R., Szema, K.Y., and Lewis, C.H., "Viscous Shock Layer Predictions for Hypersonic Laminar or Turbulent Flows in Chemical Equilibrium Over the Windward Surface of a Shuttle-Like Vehicle," AIAA Paper 82-0201, Jan. 1982.

[14] MacCormack, R.W., "A Numerical Method for Solving the Equations of Compressible Viscous Flow," AIAA Paper 81-0110, Jan. 1981.

[15] Li, C.P., "Hypersonic Nonequilibrium Flow Past a Sphere at Low Reynolds Numbers," AIAA Paper 74-173, 1974.